Astron. Astrophys. 340, 143–148 (1998)

ASTRONOMY
AND
ASTROPHYSICS

A comparison of the fast timing behaviour of 4U 1705–44 to that of 4U 1608–52 and Cygnus X-1

M. Berger and M. van der Klis

Astronomical Institute "Anton Pannekoek", University of Amsterdam and Center for High Energy Astrophysics, Kruislaan 403, 1098 SL Amsterdam, The Netherlands

Received 13 October 1995 / Accepted 18 September 1998

Abstract. We studied the fast timing behaviour of the atoll source 4U 1705–44 using the entire EXOSAT dataset, four observations covering a total of 230 000 seconds of 1–20 keV spectral and timing data. In one of the observations, 4U 1705–44 was in a low intensity "island" state and had an unusually hard spectrum. The fast timing analysis of this hard island state shows a power spectrum very similar to that of black hole candidates in the 'low state', with a flat-topped band-limited noise component that gradually steepens towards higher frequency. We perform for the first time a quantitative comparison of the timing behaviour of an atoll source in the hard island state (4U 1705–44) with that of a black hole candidate in the low state (Cygnus X-1). We also compare the power spectrum of 4U 1705–44 in the hard island state with those of the atoll source 4U 1608–52 in a similar state as reported by Yoshida et al. (1993). Our results confirm that there are similarities between the fast timing behaviour of the hard island states of these atoll sources and the low state of black hole candidates, yet we also find significant differences in power spectral parameters; the power spectra of the neutron star systems have a lower rms amplitude and are less steep. We find a trend among the neutron star power spectral properties, in the sense that the lower the centroid frequency of the fitted Lorentzian is, the higher its fractional rms amplitude, and the steeper the continuum underneath it. In our analysis we subtracted the instrumental band-limited noise component intrinsic to the EXOSAT ME that we found in our previous work on Cyg X-3, which contaminates the power spectra up to 100 Hz. We found that this component significantly affects the observed power spectra. We propose a new method to fit the power spectra of Cyg X-1 and other black hole candidates in the low state, that provides a significantly better fit than previous models.

Key words: accretion, accretion disks – stars: binaries: close – stars: individual: 4U 1705–44 – stars: individual: 4U 1608–52 – stars: individual: Cyg X-1 – X-rays: stars

1. Introduction

In 1989, Hasinger & van der Klis (1989) divided the bright low mass X-ray binaries into two groups, which they called Z sources and atoll sources after the patterns these sources trace out in the X-ray colour-colour diagram (CD). The CDs of Z sources show three branches arranged in a roughly 'Z'-shaped pattern, whereas the CDs of atoll sources show a so-called island and banana, usually arranged together in one broad, curved branch. The island state is characterized by lower count rates, much less motion in the CD and much stronger band limited noise than the banana state.

4U 1705–44 is a burst source that was classified by Hasinger & van der Klis as an atoll source. From their paper, 4U 1705–44 appears to be a special case among the atoll sources in the sense that it has a 'hard island' state (i.e., in its island state it has a harder 1–4.5 keV spectrum than in its banana state) whereas the other atoll sources which show both a banana and an island state (4U 1735–44, 4U 1636–54 and 4U 1820–30) have an island state in which the spectrum in the 1–4.5 keV band is softer than in the banana.

The island state of 4U 1705–44 can be unambiguously identified as such from its rapid X-ray variability: it shows strong ($\sim$ 20 %) band limited noise with a cutoff frequency of about 0.3 Hz in this state (Hasinger & van der Klis, 1989, Langmeier et al., 1989). 4U 1705–44 is one of the two atoll sources known to exhibit noise with such strength. The other is 4U 1608–52 (Yoshida et al. 1993).

The motivation for our present analysis is to quantitatively investigate the suspected similarity (van der Klis, 1994b) both in shape and strength of the noise component found in these two atoll sources and that in black hole candidates in the low state, which was up to now based on mostly qualitative considerations. To this aim, we re-examine the EXOSAT observations of 4U 1705–44, and perform, for the first time, a systematic, quantitative and direct comparison with 4U 1608–52 as well as with the black hole candidate Cyg X-1. An additional reason to carefully look at these data again came from our earlier work on Cyg X-3 (Berger & van der Klis, 1994) which suggested that an instrumental effect of EXOSAT contaminates the ME power spectra between 0 and 100 Hz. This effect is important for the power spectra of the banana state especially, and we show that it should be taken into account.

2. Observations

From 1983 until 1986 the instruments of EXOSAT were pointed at 4U 1705–44 four times. A log of the observations is given in

Send offprint requests to: M. Berger

Table 1. The lightcurves of the four observations are given in Langmeier et al. (1987). The labeling (a) to (d) is identical to the labeling used by these authors.

The EXOSAT ME-instrument (Turner et al. 1981, White & Peacock 1988) consisted of eight proportional X-ray counters. In the present analysis, the data from the 1–20 keV argon proportional counters are used. The data were processed on board the satellite by the On Board Computer (OBC), which had different modes emphasizing either spectral (High Energy Resolution or HER) or timing (High Time Resolution, HTR) information; the OBC modes that were used and the resulting highest time resolutions are indicated in Table 1.

The array of eight counters of the EXOSAT ME was configured in two halves of four counters each; one detector failed in 1984. The half arrays could both be pointed at the source, or either of them could be offset by tilting. In this way, background data could be obtained with one array-half, while making the observation with the other. In the rightmost column of Table 1 the number of detectors pointed at the source in different segments of each observation is indicated.

3. Analysis

3.1. Timing analysis

The timing behaviour of 4U 1705–44 was studied by making fast Fourier transforms of the high time resolution data, divided into equal length time intervals. Each time interval was checked for gaps and spikes (due to telemetry dropouts or other instrumental shortcomings). Spikes were defined as single-bin excesses over the average count rate with a probability of chance occurrence from Poisson statistics of 10^{-8} per bin. Every data segment in which a spike or gap occurred (only a few percent of the data segments) was excluded from further analysis. The data segments affected by X-ray bursts were also excluded from the analysis.

The resulting Fourier transforms were squared and Leahy normalized (Leahy et al., 1983). The first step in analyzing these power spectra was to subtract the Poisson level, a white noise level caused by counting statistics, which we took to be given by $P = 2(1 - \mu\tau_{\rm dead})^2$, with P the Poisson level, μ the detected count rate per detector, and $\tau_{\rm dead}$ an "effective" instrumental deadtime. In earlier work, we found that $\tau_{\rm dead} = 10.6\mu$s (Berger & van der Klis, 1994), and we adopted that value in the present work. We then renormalized the Poisson-level subtracted power spectra to (rms/mean)^2/Hz normalization by dividing the Leahy-normalized power spectrum by the average total observed count rate I appropriate for each spectrum (e.g.,van der Klis, 1994a).

We then constructed average power spectra. The power estimates in a power spectrum of a random process are distributed according to a chi-squared distribution with 2 degrees of freedom, with a standard deviation σ equal to the power estimate itself, and in practice the power spectra of X-ray binaries follow this distribution very well (van der Klis, 1989). So, in principle, when averaging power spectra one should perform a weighted average with weights $1/\sigma^2$. However, by doing this one would effectively be assigning each power estimate a weight equal to its inverse value squared. This would introduce a strong bias in favour of power estimates that are just statistically low, due to the bin-to-bin statistical fluctuations. Therefore, it would be preferable to estimate the weights from the *average* power at each frequency rather than from the power itself, but of course the average power is not known in advance. An acceptable procedure turns out to be in most cases to first perform an unweighted average, and use the average powers resulting from that in setting the weights for the final, weighted averaging.

In our case, we have the additional complication that the count rates I vary strongly between the data sets whose power spectra we are averaging, causing strong variations in the contribution to the total power of the Poisson counting noise, which has a value in our renormalized power spectra of approximately $P_{\rm Poiss} = 2/I$. We therefore in the first step of the averaging process used weights $1/\sigma^2_{\rm Poiss}$, where $\sigma_{\rm Poiss} \equiv 2/I$. The resulting average power spectrum, with powers $\langle P\rangle$, was used to set the final weights as $1/\sigma^2$, where $\sigma \equiv \langle P\rangle + 2/I$. These values of σ are close to the power estimates of the final averaged power spectrum, as they should be, and are much less affected by the bin-to-bin fluctuations in power than if they would have been estimated from the individual power spectra, thus avoiding biasing the result in favour of lower power estimates.

The two averaging steps described in the previous paragraph could be iterated in order to bring the estimates of σ even closer to the final powers, but this proved not to be necessary in our case. The underlying assumption is, of course, that the instrinsic source variability within each observation has a constant power spectrum, which is consistent with what can be derived from inspection of power spectra of subsets of the data. To our knowledge this method of averaging power spectra has not been previously applied in X-ray timing.

From our analysis of the fast timing behaviour of Cyg X-3 (Berger & van der Klis, 1994) it followed that it is likely that an instrumental effect contaminates the EXOSAT ME argon power spectra at high frequencies by introducing a band limited noise component with a cutoff frequency of $\sim$100 Hz and a fractional rms amplitude of $\sim$3% of the total (source + background) count rate.

In terms of a (rms/mean)^2/Hz normalized power spectrum the instrumental component was found in the Cyg X-3 data to be independent of count rate and given by $P(\nu) = 1.44 \times 10^{-5}\nu^{5.2\times10^{-2}}e^{-\nu/118.2}$, with the frequency ν in Hz. The count rates of 4U 1705–44 are all in the range of count rates considered by Berger & van der Klis (1994), and assuming the same component is present in the 4U 1705–44 data, as the Cyg X-3 analysis suggests, we subtracted this high frequency noise component from all power spectra of 4U 1705–44.

3.2. Spectral analysis

The spectral behaviour of 4U 1705–44 was studied by making X-ray colour-colour diagrams of the available HER data. To do this, the HER data were divided into four contiguous energy bands with boundaries 0.95, 2.4, 3.4, 5 and 11.6 keV. We interpolated between the original ME spectral channels in order to

Table 1. Observations of 4U 1705–44 carried out with EXOSAT

Observation	Start (Year/day, Jan 1=1, UT)	End (Year/day, UT)	OBC modes	Time resolution (1/1024 s)	Source count rate (c/s/detector)	Nr. of detectors on source
(a)	1983/211 03:49	1983/211 11:06	HER4, HTR3	8	203	4
(b)	1985/254 08:50	1985/255 13:35	HER5, HTR3	1,8	11	3,4,7
(c)	1985/276 17:30	1985/277 13:14	HER5, HTR5	1	53	3,4,7
(d)	1986/097 07:30	1986/098 01:35	HER5, HTR5	1	42	7

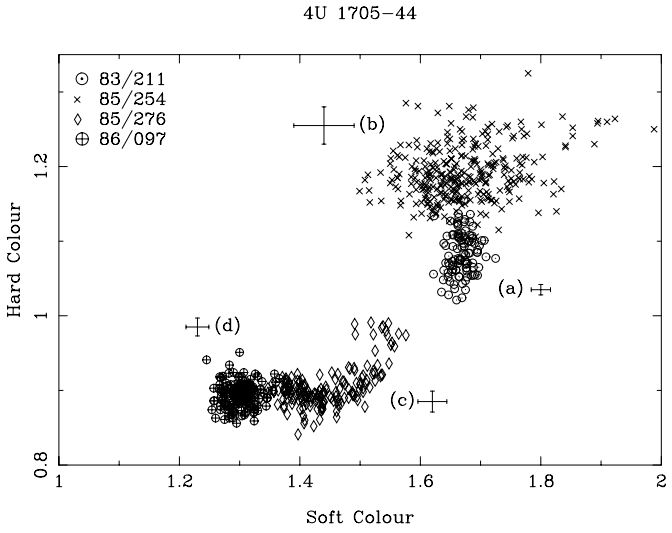

Fig. 1. The X-ray colour-colour diagram of 4U 1705–44. Indicated are the labels as defined in Table 1, and a typical error bar associated with each observation.

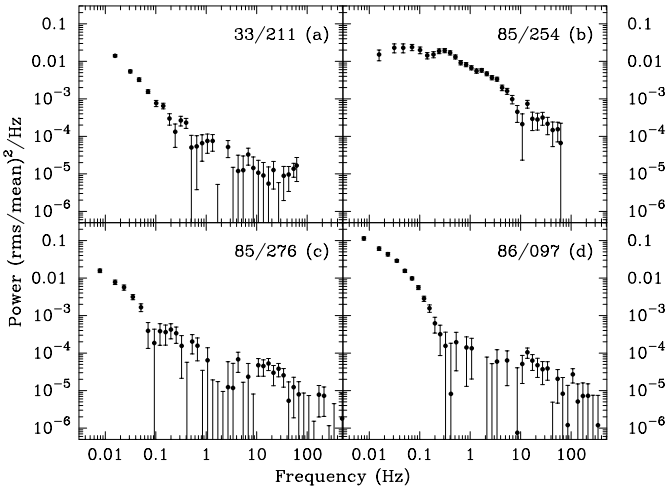

Fig. 2a–d. The average power spectra of the four observations of 4U 1705–44. The ME instrumental noise component has been subtracted in this figure.

keep these boundaries constant between observations. The ratio of the dead-time corrected and background subtracted count rates in these bands is called an X-ray colour, the soft colour being the ratio of the 2.4–3.4 and 0.95–2.4 keV count rates and the hard colour the ratio of the 5–11.6 and 3.4–5 keV count rates. We used 256 second integrations per point in the CD. The background was measured from slew data or from the offset array half.

4. Results

The colour-colour diagram of 4U 1705–44, included here for reference purposes only, is shown in Fig. 1. Different observations are drawn with different symbols.

The power spectra of the four observations are drawn in Fig. 2a–d. Observation (c) shows the source in a typical banana state, with clear very low frequency noise (VLFN) and high frequency noise (HFN) with an amplitude of only a few percent. Observation (d) appears very similar, although the VLFN could not be reliably measured (see below).

Observation (a) shows the source on a very high part of the banana, with very weak HFN, and VLFN that is stronger than in (c). Observation (b) is located at the same soft colour, but at slightly higher hard colour than (a) in the colour-colour diagram. The larger scatter of the points in the CD of observation (b) is due to the much lower count rate (see Table 1). Strong band limited noise and no VLFN are seen in this observation. In order of ascending count rate, the observations are (b) $\rightarrow$ (d) $\rightarrow$ (c) $\rightarrow$ (a). In the classic 'atoll' phenomenology, the island state has a low count rate and strong variability above 1 Hz. Observation (b) is thus classified as an island, whereas observation (a) is not.

4.1. Banana state fits

The power spectra of the banana state observations (a), (c) and (d) were fitted with a function consisting of two components: Very Low Frequency Noise and High Frequency Noise. The VLFN component was taken to be a power law $P(\nu) \propto \nu^{-\alpha_1}$. In observation (d), made in EXOSAT's last orbit before re-entry into the Earth's atmosphere, when the count rate was severely influenced by spacecraft jitter causing variations in collimator transmission, the VLFN could not be measured. The HFN component was taken to be an exponentially cut-off power law $P(\nu) \propto \nu^{-\alpha_2} \exp(-\nu/\nu_{\rm cutoff})$.

Without subtracting the instrumental component, the measured HFN rms amplitude was about 5.3% for observations (c) and (d), and about 3.2% for observation (a). The subtraction of the instrumental noise produces a significant correction to the powers measured in the 1–100 Hz range: The rms amplitudes drop to about 3.4% for observations (c) and (d), and for observation (a) now only an upper limit of 1.2% can be determined.

Table 2. Parameters of the fitted functions to the data where the ME instrumental noise component has been subtracted. The VLFN rms is measured from 0.001 to 1 Hz, the HFN rms from 1 to 100. The VLFN of observation 1986/097 could not be measured due to strong spacecraft jitter. The upper limit to HFN rms amplitude in (a) is the measured value plus three times the 1σ error obtained from the fit.

Banana state observations

Obs.	VLFN % rms	α_1	HFN % rms	α_2	$\nu_{\rm cutoff}$ (Hz)	χ^2/dof
(a)	4.2 ± 0.2	1.50 ± 0.05	< 1.2	–	∞	37.4/30
(c)	2.7 ± 0.1	1.32 ± 0.06	3.4 ± 0.4	-2.7 ± 2.0	7 ± 5	43.0/39
(d)	–	–	3.5 ± 0.4	-5.4 ± 3.3	3.2 ± 2.2	60.2/39

4.2. Island state fits

The average power spectrum of the hard island state observation (b) was fitted with two different functions: A "once broken power law" plus a Lorentzian (as used by Yoshida et al. in their analysis of 4U 1608–52), and a "twice broken power law" (as used by Belloni & Hasinger 1990 in their analysis of Cyg X-1). The power spectrum along with the fitted functions is shown in Fig. 3a and b, and the parameters of the fitted functions are shown in Table 3, where the corresponding values for 4U 1608–52 and Cyg X-1 fits were taken from Yoshida et al. (1993) and Belloni & Hasinger (1990).

For comparison, a Ginga power spectrum of Cyg X-1 in its low state (e.g. Miyamoto & Kitamoto, 1989) was fitted with the combination of the two functions: a twice broken power law plus a Lorentzian located between the two breaks. Including the Lorentzian significantly improved the χ^2 of the fit with respect to the twice broken power law fit, from 450 for 34 d.o.f. to 352 for 31 d.o.f. The fit to the low state power spectrum of Cyg X-1 with its fit is shown in Fig. 4. In Table 4 the fit results for Cyg X-1 are given.

We refer to Sect. 5 for a discussion of these results.

We investigated the properties of 4U 1705–44 in the island state further by dividing the colour-colour diagram into 3 by 3 rectangular boxes, and calculating the average power spectrum of all data within each colour box. The measured fractional rms variability from 1 to 100 Hz was consistent with being constant in all 9 boxes (the observed scatter in the 9 integrated powers was 1.77×10^{-4}, whereas the predicted scatter from the errors on the individual powers was 1.71×10^{-4}).

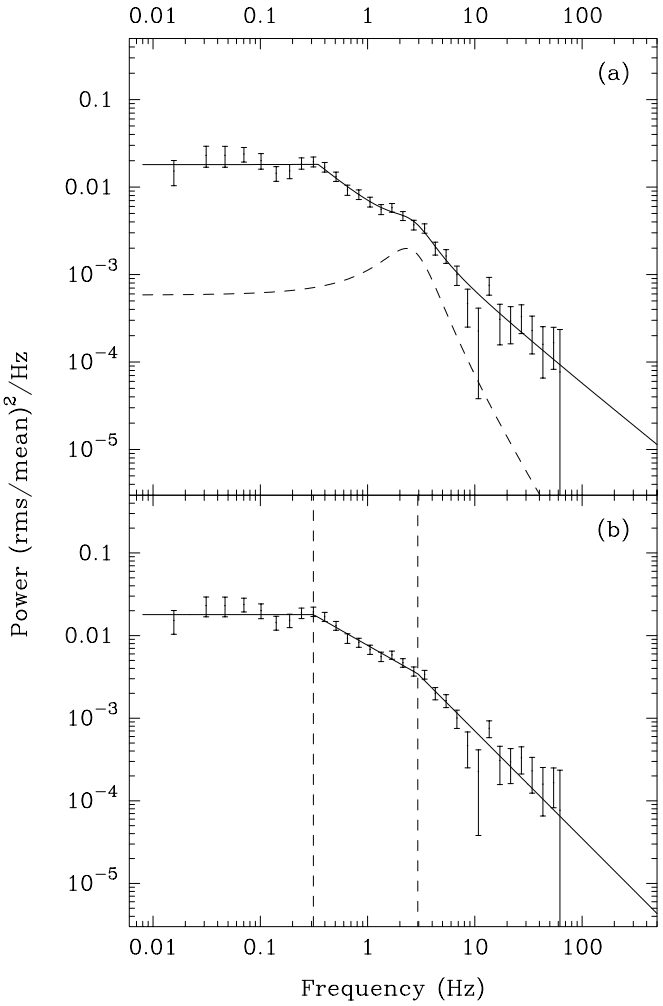

Fig. 3a and b. The power spectra of the island state of 4U 1705–44, fitted with a broken power law plus a Lorentzian near 2 Hz (top panel; the Lorentzian is indicated by dashed lines) and a three-component broken power law (bottom panel; the break frequencies are indicated by dashed lines).

5. Discussion

The power spectrum of 4U 1705–44 can be described equally well with a once broken power law plus a Lorentzian as with a twice broken power law, and above we have reported results of both fits. On the basis of the first fit, a direct comparison can be made to 4U 1608–52, as a once broken power law plus Lorentzian was fitted by Yoshida et al. (1993) to the three Ginga observations of the source in its hard island state. In this quantitative comparison, 4U 1705–44 turns out to be indeed quite similar to 4U 1608–52. The break frequency in 4U 1705–44 (0.35 Hz) is in the range of those found in 4U 1608–52 (0.2–1.0 Hz). The power law slope of 4U 1705–44 is a bit steeper (1.0 vs. 0.8–0.9) and the Lorentzian has a centroid at somewhat lower frequency (2.3 vs. 5–9) than in 4U 1608–52, and a somewhat higher rms amplitude (~ 9 vs. 4–7 %). There is some evidence for a trend in the sense that the lower the centroid frequency of the Lorentzian is, the higher its fractional rms amplitude, and the steeper the continuum underneath it; this holds not only between the two sources, but also between the three separate observations of 4U 1608–52.

Table 3. Left column: Parameters of the fitted once broken power law + Lorentzian *(top)* and the twice broken power law *(bottom)* to observation (b) of 4U 1705–44. Right column: Corresponding parameters for 4U 1608–52 (Yoshida et al. 1993) and Cyg X-1 (Belloni & Hasinger, 1990).

Once broken power law + Lorentzian

Parameter	4U 1705–44	4U 1608–52
Broken power law integral (.01-100 Hz)	$(4.0 \pm 0.4) \times 10^{-2}$	$(3.2 - 9.6) \times 10^{-2}$
Break frequency $\nu_{\rm break}$(Hz)	0.35 ± 0.05	0.2 – 1.0
Broken power law index, $\nu < \nu_{\rm break}$	0.05 ± 0.07	0 (fixed)
Broken power law index, $\nu > \nu_{\rm break}$	1.01 ± 0.05	0.8 – 0.9
Lorentzian integral power	$(9.4 \pm 3.5) \times 10^{-3}$	$(2 - 6) \times 10^{-3}$
Lorentzian centroid frequency (Hz)	2.3 ± 0.4	5.1 – 9.0
Lorentzian FWHM (Hz)	3.0 ± 0.9	4.5 – 6.1
χ^2/d.o.f.	20.3/25	1–1.6

Twice broken power law

Parameter	4U 1705–44	Cyg X-1
Rms integral (%)	21.3 ± 0.7 (0.03-64 Hz)	28 – 48 (0.016 – 4 Hz)
Low power law index	0 (fixed)	-0.4 – +0.2
Low break frequency (Hz)	0.31 ± 0.04	0.05 – 0.35
Intermediate power law index	0.74 ± 0.06	0.9 – 1.4
High break frequency (Hz)	3.0 ± 0.6	1.2 – 5.8
High power law index	1.34 ± 0.15	1.4 – 2.4
χ^2/d.o.f.	27.1/27	1.1 – 3.7

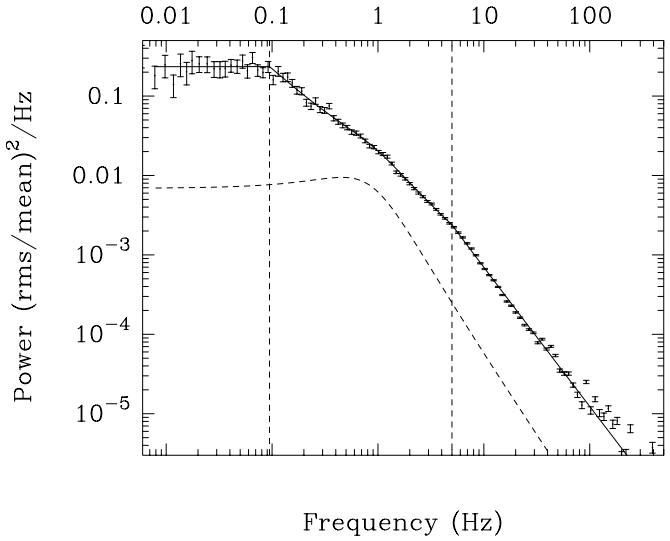

Fig. 4. The power spectrum of Cyg X-1 in its low state, fitted with a twice broken power law plus a Lorentzian near 0.5 Hz. The break frequencies are indicated by vertical dashed lines; the Lorentzian component is indicated separately as well.

We find that the power spectrum of Cyg X-1 can be significantly better described with a twice broken power law plus an additional Lorentzian than by just a twice broken power law. Comparing our fit of a twice broken power law plus Lorentzian with the fits of Belloni & Hasinger (1990) to Cyg X-1 power spectra of just a twice broken power law, one sees that the two break frequencies we find, at 0.1 Hz and 5 Hz, are both in the range of the break frequencies they find (0.05–0.35 and 1.2–5.8 Hz). The additional Lorentzian we fit in the power spectrum of Cyg X-1 is centered at 0.4 Hz, in between the breaks. This suggests that the Lorentzian describes additional structure in the power spectrum, located between the two break frequencies, and does not strongly affect the basic continuum shape described with the twice broken power law. We note that the black hole candidate J0442+32, as observed with OSSE (Grove et al. 1994) shows, in the 35–175 keV band, very clear evidence for the presence of a peak at a similar frequency (0.23 Hz), superimposed on a similar band limited noise continuum (see Grove et al. 1994, Fig. 2).

Table 4. Parameters of the fitted twice broken power law + Lorentzian to the power spectrum of Cyg X-1 in its low state.

Cyg X-1: Twice broken power law + Lorentzian

Parameter	Value
Low power law index	0 (fixed)
Low break frequency (Hz)	$(9.5 \pm 0.6) \times 10^{-2}$
Intermediate power law index	1.18 ± 0.02
High break frequency (Hz)	5.00 ± 0.15
High power law index	1.73 ± 0.01
Lorentzian integral power	$(2.3 \pm 0.7) \times 10^{-2}$
Lorentzian centroid frequency (Hz)	0.42 ± 0.16
Lorentzian FWHM (Hz)	1.50 ± 0.13
χ^2/d.o.f.	352/51

To compare 4U 1705–44 to Cyg X-1, we need make an assumption about the nature of the correspondence between the power spectral fits to the two sources. Within the statistics, the data allow the following two possibilities:

(i) The two break frequencies found in the twice broken power law fit of 4U 1705–44 (at 0.3 and 3 Hz) correspond to the two break frequencies found in Cyg X-1, which are at similar frequencies: in our fit at 0.1 and 5 Hz and in the fits of Belloni & Hasinger in the ranges 0.05–0.35 Hz and 1.2–5.8 Hz.

(ii) The Lorentzians and break frequencies found in the once broken power law plus Lorentzian fits of 4U 1705–44 and 4U 1608–52 (centroids 2.3 Hz and between 5 and 9 Hz, breaks 0.35 Hz and 0.1–1 Hz, respectively) correspond to

the Lorentzian and lower break we find in Cyg X-1 (centroid 0.4 Hz, break 0.1 Hz). Clearly, in this case the centroid and break frequencies are lower in Cyg X-1 than in the two neutron stars; also the strength of the Lorentzian (15%) is larger.

In the first case, the implication is that the Lorentzian is missing from the 4U 1705–44 fit. We cannot exclude that such a component is present between the two breaks in 4U 1705–44, but it cannot have the same fractional rms amplitude as that seen in Cyg X-1: the 3 σ upper limit is 8.8%, whereas the amplitude of this component in Cyg X-1 is 15%. This means that the "equivalent width" (amplitude as fraction of continuum amplitude) could be approximately the same as in Cyg X-1. In the second case, the implication is that in 4U 1705–44 we have not yet seen the high frequency break. We investigated the possibility of the presence of such an additional break in the power spectrum of 4U 1705–44 using the one EXOSAT observation which had a 0.25 ms time resolution, but the complicated dead time effects of EXOSAT in this mode (see Tennant 1987) and limited statistics prevented us to constrain the power spectral shape sufficiently well to reach definite conclusions.

Two conclusions can be drawn irrespective of whether interpretation (i) or (ii) is true: the neutron star power spectra are less steep, and correspond to a lower fractional amplitude than those of Cyg X-1. If (i) the break frequencies of 4U 1705–44 can be identified with those in Cyg X-1, then the power law index between the two breaks is 0.7 in 4U 1705–44 vs. 0.9–1.4 in Cyg X-1, and above the high break frequency 1.3 vs. 1.4–2.4 in Cyg X-1. In case (ii) the power law index above the break is 0.8–0.9 and 1, respectively, in 4U 1608–52 and 4U 1705–44, to be compared with 1.2, steepening further out to 1.7, in Cyg X-1. For 4U 1705–44 the fractional rms amplitude of the variability is about 21% (between 0.01 and 100 Hz), and for 4U 1608–52 18–30% (Yoshida, 1993). For Cyg X-1 it is nearly always higher: 28-48% (integrated over a smaller frequency interval, 0.016–4 Hz) (Belloni & Hasinger, 1990).

Note that in interpretation (ii) Cyg X-1 extends the trend that was noted above to exist between 4U 1705–44 and the three observations of 4U 1608–52: lower Lorentzian frequency corresponds to higher Lorentzian amplitude and a steeper continuum.

So, comparing the two atoll (neutron star) sources to the black hole candidate Cyg X-1 we find that all these sources have power spectra that are similar in the sense that they become steeper towards higher frequency and have fractional rms amplitudes of a few times 0.1. However, the power spectrum of Cyg X-1 is nearly always significantly steeper than that in the neutron stars, and the rms amplitude of the power spectrum is nearly always larger. Similar conclusions probably apply to other BHC's in the low state, which have power spectral characteristics similar to those of Cyg X-1 (see Miyamoto et al. 1992)

6. Conclusion

We studied the similarities in the fast timing behaviour of two atoll sources in hard island states, and of the black hole candidate Cyg X-1 in its low state. In addition to confirming the similarities discussed previously (van der Klis 1994b and Yoshida 1993), we performed for the first time a quantitative comparative analysis of the power spectral features, which showed that the power spectra of the neutron stars were less steep and had a smaller rms amplitude than that of Cyg X-1.

Limited statistics prevent us to confirm or reject the presence of an additional Lorentzian component at lower frequencies (0.3–3.0 Hz) in the power spectrum of 4U 1705–44, or an additional steepening of the continuum towards higher frequency, at least one of which would be predicted on the basis of the analogy to Cyg X-1. Observations with future satellites with a larger effective area and faster sampling speed (like XTE) are required to obtain a more complete picture of the similarities and differences between the fast timing of black hole candidates in their low states and atoll sources in hard island states.

Acknowledgements. This work was supported in part by the Netherlands Organization for Scientific Research (NWO) under grant PGS 78-277.

References

Andrews D., Stella L., 1985, EXOSAT Express 10, 35
Berger M., van der Klis M., 1994, A&A 292, 175
Belloni T., Hasinger G., 1990, A&A 227, L33
Grove J.E., et al., 1994, in: The Second Compton Symposium, Fichtel C.E, Gehrels N., Norris J.P. (eds.), AIP Conference Proc. 304, 192
Hasinger G., van der Klis M., 1989, A&A 225, 79
Van der Klis M., 1989, in: Timing Neutron Stars, H. Ögelman, E.P.J. van den Heuvel (eds.), Kluwer Academic Publishers, p. 27
Van der Klis M., et al., 1990, ApJ 360, L19
Van der Klis M., 1994a, in Proc. NATO ASI Lives of the neutron stars, Aug–Sep 1993, Kemer, Turkey.
Van der Klis M., 1994b, ApJS 92, 511
Langmeier A., Sztajno M., Hasinger G., Trümper J., 1987, ApJ 323, 288
Langmeier A., Hasinger G., Trümper J., 1989, ApJ 340, L21
Leahy D.A., Darbro W., Elsner R.F., et al., 1983, ApJ 266, 160
Miyamoto S., Kitamoto S., 1989, Nat 342, 773.
Miyamoto S., Kitamoto S., Iga S., Negoro H., Terada K., 1992, ApJ 391, L21
Tennant A.F., 1987, MNRAS 226, 963
Turner M.J.L., Smith A., Zimmerman H.U., 1981, Space Sci. Rev. 30, 513
White N.E., Peacock A., 1988, in *X-ray Astronomy with EXOSAT*, R. Pallavicini & N.E. White (eds.), Mem. S. A. It. 59, 7
Yoshida K., Mitsuda K., Ebisawa K., et al., 1993, PASJ 45, 605